Materials Transactions, Vol. 47, No. 7 (2006) pp. 1631 to 1637
Special Issue on Thermal Spraying

In-Situ Densification of Ti Coatings by the Warm Spray (Two-Stage HVOF) Process

Jin Kawakita[1], Seiji Kuroda[1], Sebastian Krebs[2,*] and Hiroshi Katanoda[3]

[1]*Thermal Spray Group, Materials Engineering Laboratory, National Institute for Materials Science, Tsukuba 305-0047, Japan*
[2]*Department of Mechanical Engineering, Helmut Schmidt University, Hamburg D-22043, Germany*
[3]*Department of Mechanical Engineering, Kagoshima University, Kagoshima 890-0065, Japan*

Coating of titanium is one of the surface modification techniques attractive for corrosion protection in various industrial and medical applications. *In-situ* densification of titanium coatings fabricated by the Warm Spray (two-stage high velocity oxy-fuel (HVOF)) process was investigated for the purpose of obtaining impermeability together with minimum oxidation level. Ceramic beads of ZrO_2-SiO_2 were mixed with titanium feedstock powder. By the peening effect of the ceramic particles the density of the resultant titanium-matrix coatings could be improved and the minimum coating porosity obtained in this study was 0.65 vol%. [doi:10.2320/matertrans.47.1631]

(Received December 26, 2005; Accepted March 16, 2006; Published July 15, 2006)

Keywords: *Warm Spray, titanium, ZrO_2-SiO_2, peening effect, porosity*

1. Introduction

Titanium (Ti) is one of very attractive materials for industrial and medical applications because of its high corrosion resistance and biocompatibility. Coating of Ti has been investigated for many years and it is clear that the coating density is essential for protection of the substrate from corrosion. In addition, coating's oxidation should be kept minimum as it is also useful for the manufacturing processes such as machining and bending.

Although low-pressure plasma spraying is capable of making such high quality coatings,[1)] it has problems of high cost and limited applicability. In the air, affinity of Ti with oxygen hinders deposition of pure Ti because of preferential formation of oxides. Recently, Cold Spray technique was reported to make relatively high quality coatings of Ti. However, the density is not enough.[2)]

The Warm Spray (two-stage high velocity oxy-fuel (HVOF)) process was developed in our group and relatively dense Ti coatings could be obtained if the spray condition is set to an appropriate one.[3)] This process is equipped with a mixing chamber between the combustion chamber and the powder feeding ports. The combustion gas generated within the combustion chamber is mixed with additional inert gas such as nitrogen in order to form a supersonic jet with a lower temperature. The lowered gas temperature was remarkably effective in controlling the oxygen pickup by the sprayed powder while achieving packing density of the stacking particles higher than 98 vol%. In addition, another notable characteristic of Warm Spray process of Ti is the high deposit efficiency close to 100%. To improve further the coating density while keeping the low oxidation level, a secondary material with peening function was mixed with the Ti feedstock powder. The peening effect has been reported regarding the kinetic spray processes including HVOF and Cold Spray, which enable spray particles to be deposited by the impact energy. Although the peening effect on the mechanical properties of the resulting coatings was mentioned in both cases of HVOF[4–6)] and Cold Spray,[5,7)] the relation between the peening effect and the coating density was unclear. Addition of the secondary material to the feedstock was studied on the Cold Spray.[8)] In the paper, although stacking behaviour of Al as the primary soft material was changed by introduction of Al_2O_3 and SiC as the secondary hard materials, densification was not cited. In this study, ZrO_2-SiO_2 beads were selected as the secondary peening material, which is commercially available and galvanic corrosion between different metals should not induce because the formed coating is expected to contain such a secondary phase. The particle size and content of ceramic beads was varied and their effect on densification was investigated in this paper.

2. Experimental

2.1 Spray materials and conditions

The feedstock for spraying was mixtures of pure Ti powder (Sumitomo Titanium, TILOP) in a particle size under 45 μm and fused beads of ZrO_2-SiO_2 (Macoho, Zirblast B-series) in a size distribution of 63–125, 125–250 and 425–600 μm. The chemical compositions of Ti and ceramic beads are listed in Table 1. The percentage of ceramic beads within the mixtures was 0, 10 and 50 mass%.

Spray conditions are listed in Table 2. To clarify the effect of additional ceramic on *in-situ* densification of the coatings, the condition A was applied for spraying because the Ti coating had been obtained with 3.55 vol% in porosity and with 0.5 mass% in oxygen content.[3)] Spraying was also carried out under the condition B, which had given the Ti

Table 1 Chemical compositions of feedstock powders.

Material	Composition (mass%)
Ti (Sumitomo Ti, TILOP, −45 μm)	Ti bal, Fe 0.031, O 0.141, C 0.007, N 0.011, H 0.007
Ceramic beads (Macoho Zirblast)	ZrO_2 67, SiO_2 30, Others 3 (Al_2O_3, Fe_2O_3 and TiO_2)

*Undergraduate Student, Helmut Schmidt University

Table 2 Spray conditions.

	A	B
Kerosene flow rate ($dm^3 \cdot min^{-1}$)	0.30	0.35
O_2 flow rate ($m^3 \cdot min^{-1}$)	0.623	0.708
N_2 flow rate ($m^3 \cdot min^{-1}$)	1.5	1.0
Spray distance (m)	0.10	0.18
Scan speed ($m \cdot s^{-1}$)	0.7	
Pitch width (mm)	4	
Powder feed rate ($g \cdot min^{-1}$)	38	

coating in a lower porosity of 1.87 vol% but with twice more oxygen content than condition A. The substrate was carbon steel JIS SS400 with the dimensions of $5 \times 50 \times 100$ mm. The substrate was blasted with alumina grits and degreased ultrasonically in acetone prior to spraying. In all the spray cases, the backside of the substrate was cooled by blowing the compressed air at a flow rate of $0.3\ m^3 \cdot min^{-1}$.

Temperature of the target surface during spraying was measured with the thermo-couple fixed into the vertical hole with 1 mm in diameter at a distance within 1 mm from the substrate surface faced to the spray gun.

2.2 Coatings characterisation

Surface and cross section of the coated specimen were examined by scanning electron microscopy (SEM, JEOL JSM-5400) with energy-dispersive X-ray spectroscopy (EDX). The cross section was also observed by the optical microscope (Olympus, BX60M). The cross section was prepared by ordinary metallographic technique, *i.e.* embedding the coated specimen into an epoxy resin, followed by grinding and polishing treatments.

The open porosity of the coatings was determined by mercury intrusion porosimetry with the apparatus of Micromeritics Autopore II 9220.

The chemical composition was determined by the inert-gas fusion method for oxygen, by ICP-AES for Ti, Zr, Fe and Al, and by gravimetry for Si by evaporation to dryness of SiO_2 with the white smoke treatment by pechloric acid.

Polarisation resistance of the coated specimen was evaluated by the polarization and the alternating current (AC) impedance methods. The detailed procedure was described elsewhere.[9] The working and the counter electrodes were the coated specimen, the sprayed area of which was left exposed with $2\ cm^2$ and the rest of the specimen surface was insulated with silicone resin. The reference electrode was the Ag/AgCl electrode in the saturated KCl solution. The electrolyte was artificial seawater of pH8.3 at 300 K. The corrosion potential was also measured with the same electrochemical cell.

Hardness of the coatings was measured using the micro Vicker's hardness tester (MVK-E, Akashi Co.). Microhardness measurements of the coatings were made with a 0.98 N load keeping for 15 seconds at room temperature.

3. Results and Discussion

Figure 1 shows a typical appearance of the coating surface observed by SEM and elemental maps analyzed by EDX. Through this paper, experimental results are shown concerning the coated specimens prepared under the condition A unless the coating condition is specified. Almost all the surface was covered with Ti particles. The content of ceramic

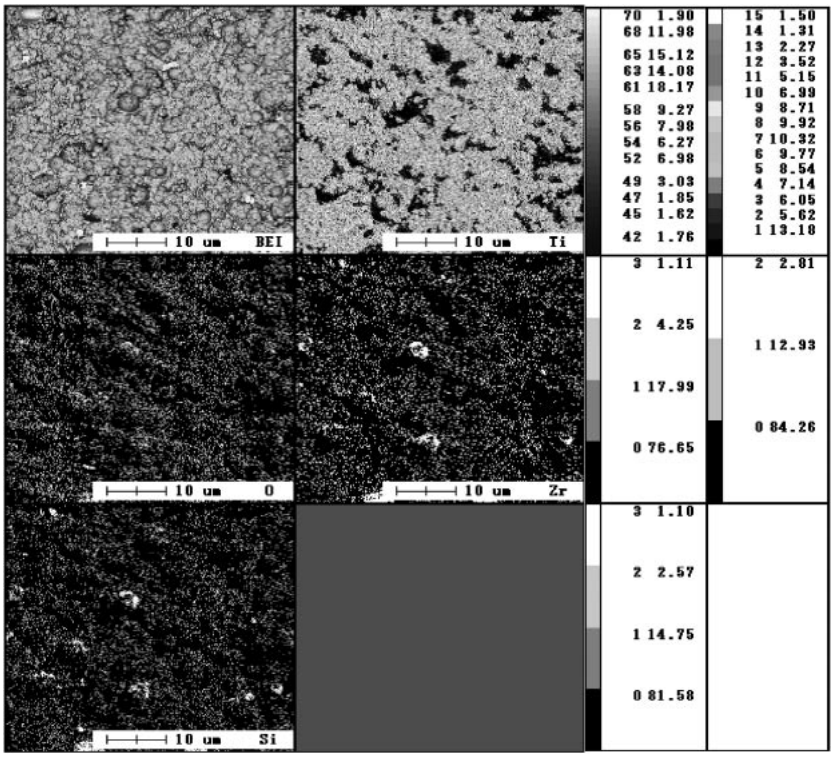

Fig. 1 SEM image of coating surface of Ti and ZrO_2-SiO_2 composite and its elemental mapping by EDX. ZrO_2-SiO_2 is 50 mass% in feedstock and 63–125 μm in particle size.

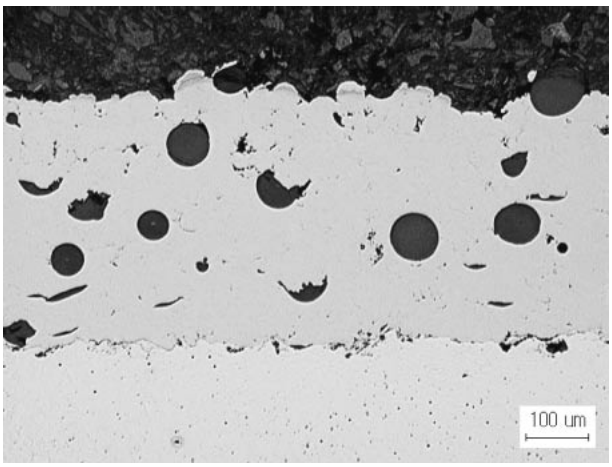

Fig. 2 Cross sections of composite coating of Ti and ZrO_2-SiO_2. ZrO_2-SiO_2 is 50 mass% in feedstock and 63–125 μm in particle size.

particles detected as Zr or Si was much smaller than the nominal mixture ratio.

Figure 2 shows a typical cross sectional image of the coating observed by optical microscopy. Some dimples were found near the top layer of the coating. These dimples and the smaller content of ceramic near the surface indicate rebounding of ceramic particles from the target after impingement. In the bottom layer near the interface between the coating and the substrate, few ceramic particles were observed because of poor adhesion between the ceramic particles and the substrate. In the middle layers of the coating, the ceramic particles were distributed homogenously. Some of the ceramic particles stacked in the coating are fractured. Figure 3 shows a typical back scattered electron image and elemental maps of the coating's cross section, observed by SEM and analyzed by EDX, respectively. Some cracks can be seen in the ceramic particle. These facts are believed to be due to impingement of subsequent sprayed particles to the brittle ceramic particle deposited on the target. In addition, no obvious pores and voids were observed beneath the ceramic particle in Fig. 3, implying effective densification of Ti matrix of the coating by the peening ceramic particles.

Figure 4 shows the dependence of actual content of ceramic beads on the particle distribution and percentage of ceramic beads in the feedstock. At the same size distribution, the actual content of ceramic beads is increased with the percentage in the feedstock. This is because the relative ratio of the impacting ceramic particles was increased. The significantly smaller actual content of the ceramic beads than the percentage in the feedstock is due to tendency of rebounding of the ceramic particles on the target without depositing.

The composite coatings in this study had difficulty in

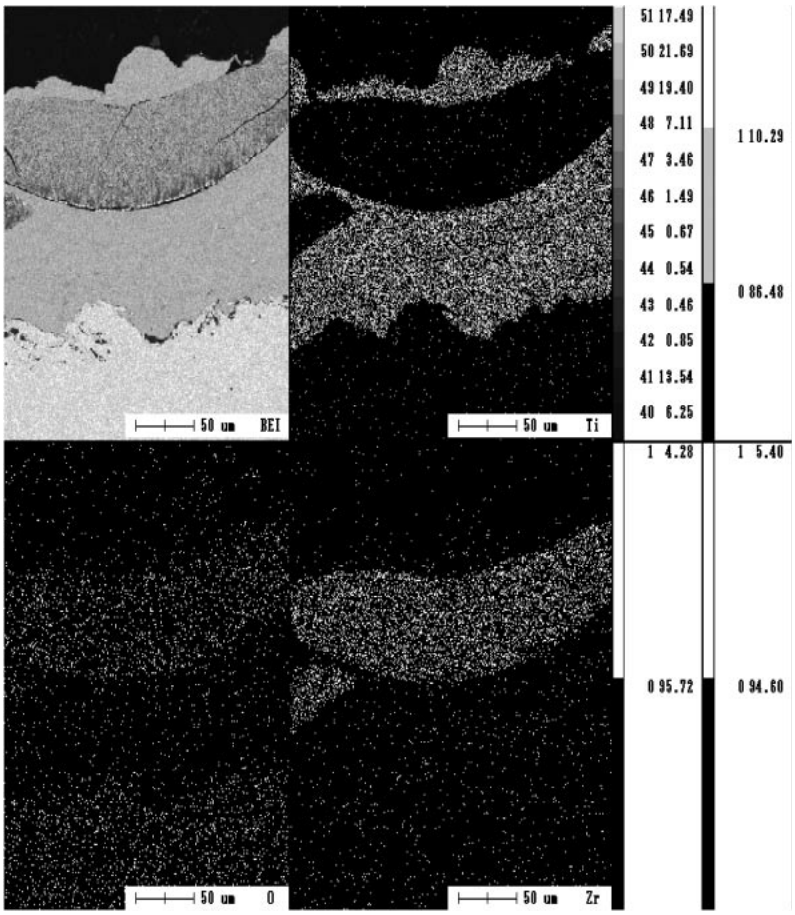

Fig. 3 Back scattered electron image and elemental map of cross section of composite coating of Ti and ZrO_2-SiO_2. ZrO_2-SiO_2 is 50 mass% in feedstock and 400–625 μm in particle size.

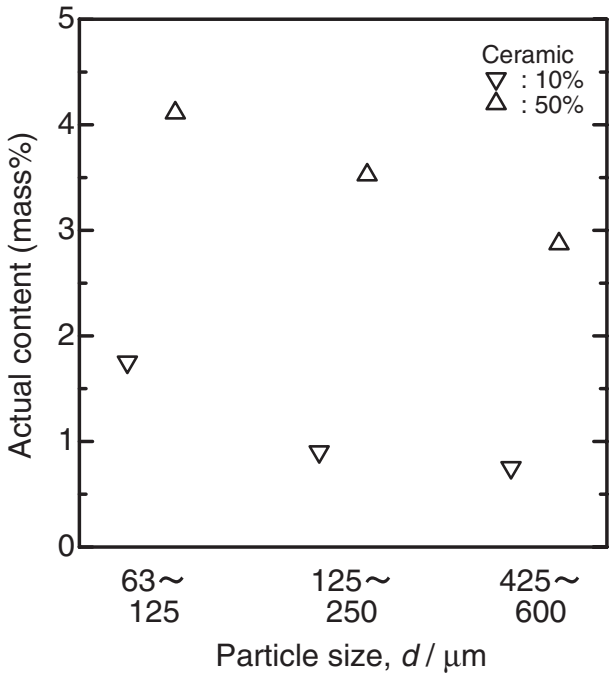

Fig. 4 Dependence of actual content of ceramic particle in coatings of Ti and ZrO_2-SiO_2 composite on size distribution and percentage of ceramic in feedstock.

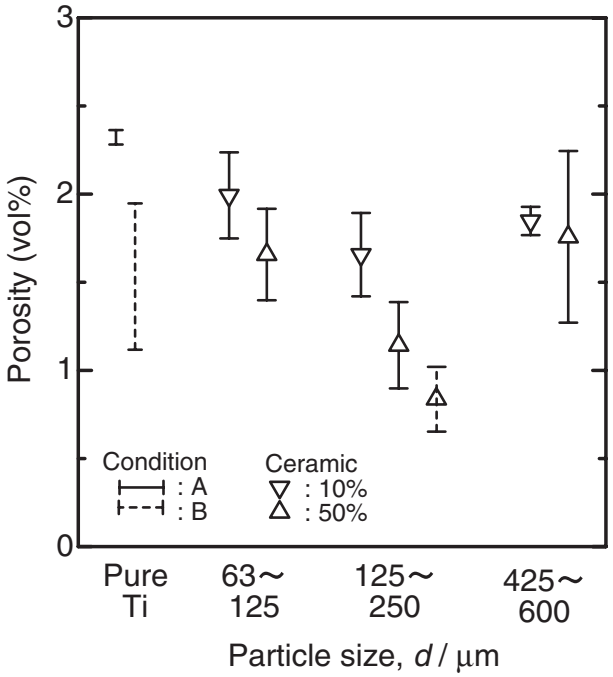

Fig. 6 Dependence of coating porosity of Ti and ZrO_2-SiO_2 composite on size distribution and percentage of ceramic in feedstock. Coatings were prepared under different spray conditions.

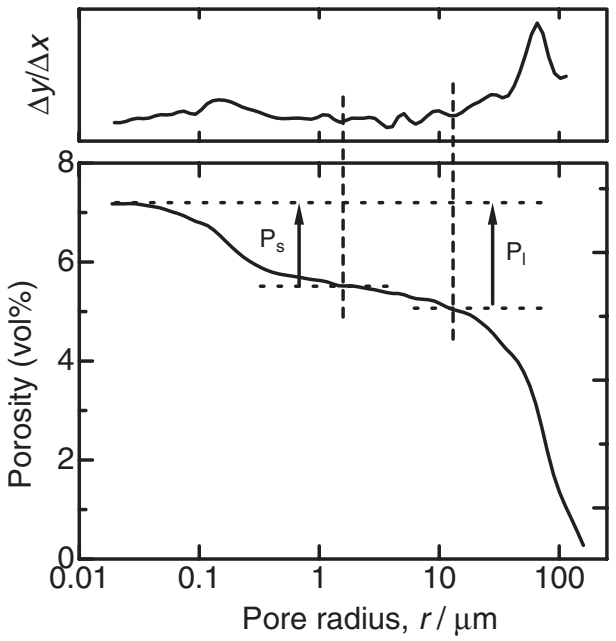

Fig. 5 Cumulative porosity as function of pore radius of Ti and ZrO_2-SiO_2 composite coating. ZrO_2-SiO_2 is 50 mass% in feedstock and 125–250 μm in particle size. Upper curve shows differentiation of lower one. P_s and P_l are porosity of the coating estimated small and large, respectively.

determining the porosity. Figure 5 shows a typical result of porosimetry of the coating. In general, a stepwise curve is obtained and the region below the second step (obvious plateau) can be assigned to the surface roughness of the specimen and be cut away when the coating porosity is calculated. As seen in Fig. 5, however, the second step goes downward. The region, in which differential values of the original date were comparatively small, was defined. By taking into account such a region, both small and large porosity were determined concerning one coating. The coating porosity is indicated as the extent between the small and the large values below. Figure 6 shows the dependence of the coating porosity of Ti and ZrO_2-SiO_2 composite on the size distribution and the percentage of the ceramic powder in the feedstock. As the particle size of ceramic was increased to the range of 125–250 μm, the coating porosity decreased at the same percentage of ceramic beads. This must be due to enhancement of the peening function of ceramic to the target during spray process. Beyond the range of 125–250 μm, the coating porosity became slightly larger. This is considered to be related to the impacting energy of the ceramic particles, derived from the kinetic energy, as discussed below. The packing density of the coating was increased with the percentage of ceramic beads. As shown in Fig. 6, by combination of mixed powder containing 50 mass% ZrO_2-SiO_2 in 125–250 μm diameter with the spray condition B suitable for fabricating denser coatings, the density of the Ti-matrix composite coating was further decreased to 0.65 vol%.

Figure 7 shows the relation between the porosity and the polarisation resistance of the coated specimens after immersion in artificial seawater for 3 days when the latter reached the constant values as plotted. Ti has so high corrosion resistance that the polarisation resistance of the coated specimen depends predominantly on the corrosion rate of the carbon steel substrate attacked through pores in the coatings. When the through-porosity of the coating is decreased, the polarisation resistance proportional to the reciprocal of the corrosion rate increased because the corrosion rate of the steel substrate per nominal surface area decreased. The

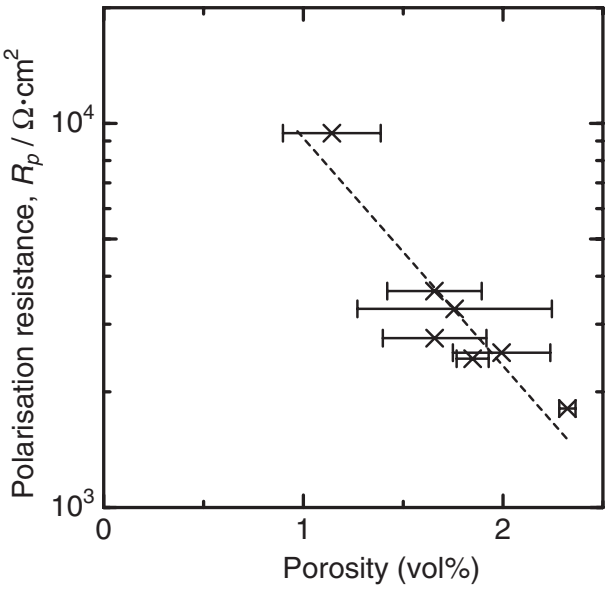

Fig. 7 Relation between porosity and polarisation resistance of Ti and ZrO_2-SiO_2 composite coatings on size distribution and percentage of ceramic in feedstock. Carbon steel JIS SS400 is used as substrate for measurement of polarisation resistance.

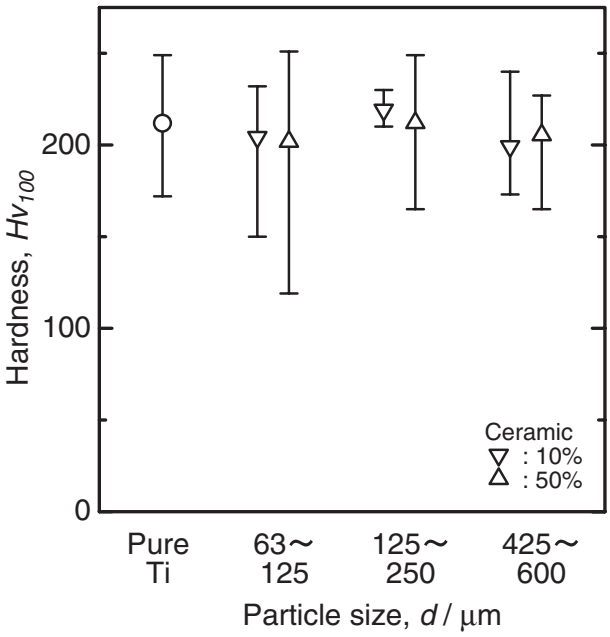

Fig. 9 Dependence of Vicker's hardness of Ti and ZrO_2-SiO_2 composite coatings on size distribution and percentage of ceramic in feedstock.

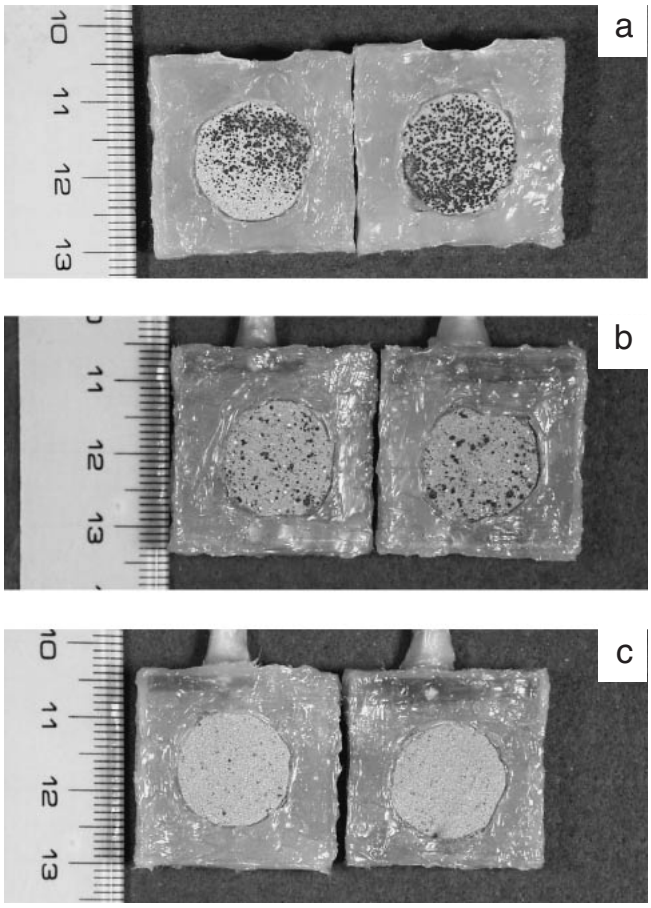

Fig. 8 Appearance of coating surface of Ti and ZrO_2-SiO_2 composite after immersion in artificial seawater for 3days with size distribution and percentage of ceramic in feedstock, a) pure Ti, b) 400–625 μm and 50 mass% and c) 125–250 μm and 50 mass%. Carbon steel JIS SS400 is used as substrate.

corrosion potential of the coated specimens showed a similar dependence on the porosity as observed in the polarisation resistance. As shown in Fig. 8, appearance of the sample surface after immersion can recognise the relation between the through-porosity of the coating and the corrosion rate of the steel substrate. The smaller amount of corrosion products on the specimen surface was in agreement with the higher polarisation resistance. Therefore, the results of the corrosion test can be used as an indicator for comparing the packing density of the coatings directly.

These results revealed that the ceramic particles with 125–250 μm in size as additional powder was most effective to densify the Ti-matrix in a coating. In order to densify the coating by the peening effect, it is necessary for the stacked particles to be deformable and for the impacting particles to have the high kinetic energy. In fact, the kinetic energy was reported to have correlation with the peening intensity.[10)]

Figure 9 shows Vicker's hardness of the specimen. The results are plotted as the averages with error bars indicating maximum and minimum values of 9 indents of which were made for three times at the three positions of polished cross section along the vertical direction to the coating face. All the composite coatings show no obvious dependence of the hardness on the size distribution and the percentage of ceramic beads in the feedstock and the values are comparable to the pure Ti coating. The measured target temperature during spraying reached around 700 K. It was reported that yield stress of Ti is 550 MPa at 294 K and 145 MPa at 700 K.[11)] These results indicate that the stacked Ti particles have thermal activation energy enough for movement of dislocation, implying they might become considerably soft during spraying in this study.

Regarding the kinetic energy of the in-flight spray particles, the energy per one particle is given by the following equation.

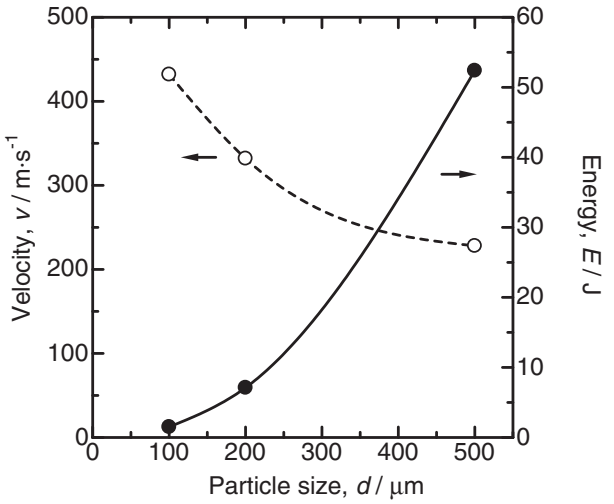

Fig. 10 Dependence of velocity and kinetic energy of one ZrO_2-SiO_2 particle on its size at exit of barrel of spray apparatus, calculated through gas dynamic simulation.

$$E = \frac{1}{2}mv^2 = \frac{1}{2}\left(\frac{4}{3}\pi\left(\frac{d}{2}\right)^3\rho\right)v^2 \quad (1)$$

E: kinetic energy, m: mass, v: velocity, d: diameter, ρ: density.

A larger ceramic particle is heavier and thus its velocity might be lower at the target position. For the kinetic energy, however, the loss in velocity might be compensated by the increase in mass. Gas dynamics modelling of the flow field of the gas in the spray apparatus as well as the acceleration of ZrO_2-SiO_2 ceramic particle injected from the powder feed ports were conducted according to the modelling method reported in detail elsewhere.[12] Figure 10 shows the dependence of the calculated velocity of one ceramic particle on its size at the exit of the barrel of the spray apparatus, superimposing the corresponding kinetic energy. From this calculation, even though the maximum velocity attained by the Warm Spray apparatus decreases with the size of ceramic particle, the kinetic energy of one ceramic particle increases with the particle diameter of 100 to 500 μm. In addition, the number of impacts by sprayed particles per unit area (coverage) must be taken into account. The total amount of kinetic energy exerted by sprayed particles onto a unit area of substrate can be expressed by

$$E_{acc} = E \times N = \frac{1}{2}\left(\frac{4}{3}\pi\left(\frac{d}{2}\right)^3\rho\right)v^2N \quad (2)$$

E_{acc}: accumulated kinetic energy, N: impact number,

where N denotes the total number of impacts by sprayed particles onto a unit area of substrate from the beginning to the end of spraying. Figure 11 shows dependence of the impact number N of Ti and ZrO_2-SiO_2 spray particles on the size distribution and the percentage of ceramic in the feedstock. The plots shows the average number of particles impinging at the same position per one pass of gun movement calculated by dividing the total area which would be covered by the sprayed powder particles spread in a single layer by

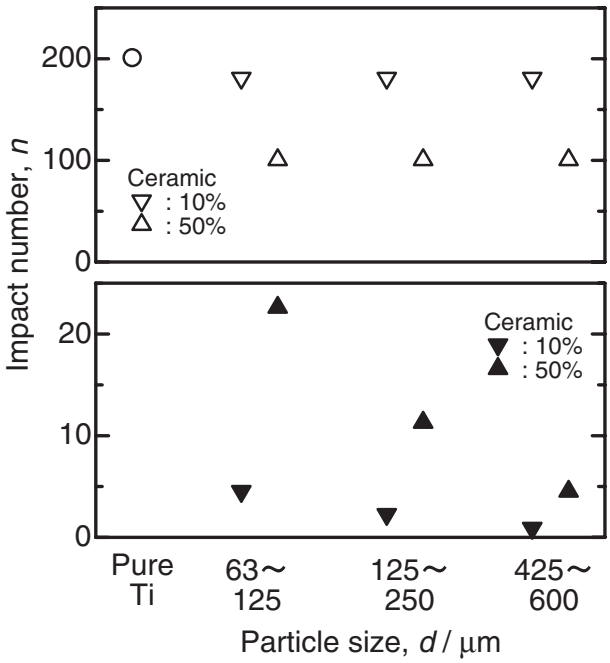

Fig. 11 Dependence of impact number of spray particles (upper: Ti and lower: ZrO_2-SiO_2) on size distribution and percentage of ceramic in feedstock. Counts are calculated at same position per one path of gun movement.

the surface area of the substrate. The impact number decreased with the particle size and with the percentage of the ceramic beads in the feedstock. Therefore, the accumulated kinetic energy might depend on the balance of kinetic energy per one impact particle and the impact number. The minimum porosity, *i.e.* the maximum density of the coatings prepared with 125–250 μm in size distribution of ceramic particles is presumably due to the optimised contribution of both increased kinetic energy and decreased impact number to densification in this study.

4. Conclusions

The density of Ti coatings fabricated by the Warm Spray process could be improved by using mixing powder of Ti and ZrO_2-SiO_2 as the feedstock. The most effective mixture for densification contains 50 mass% of ceramic particles in a size distribution of 125–250 μm.

The ceramic particle is believed to provide the peening effect during deposition by striking the coating surface followed by rebounding from and pressing of the target. This effect should have increased with the particle size, however, too large particles tended to decrease the coating density. There might be a balance between the increasing kinetic energy of one particle and decreasing impacting number to the target surface.

The minimum coating porosity attained in this study was 0.65 vol%.

The ceramic beads rebounded from the target might be reusable, but they must be checked by microscopic observation and sieved prior to reuse as the feedstock because some of them might be fractured upon impingement.

Acknowledgements

The authors are grateful to Mr. M. Komatsu for his sincere experimental works and supports.

The analytical department in NIMS was appreciated with the precise chemical analysis.

Helmut-Schmidt University is thanked for the financial support of Mr. S. Krebs.

Dr. M. Watanabe is acknowledged for his helpful discussion and advice.

REFERENCES

1) H. D. Steffens, E. Erturk and K. H. Busse: J. Vac. Sci. Technol. A **3** (1985) 2459–2463.
2) J. Karthikeyan, C. M. Kay, J. Lindeman, R. S. Lima and C. C. Berndt: Proc. 1st Int. Therm. Spray Conf., (ASM Int., 2000) pp. 255–262.
3) J. Kawakita, T. Fukushima, S. Kuroda, H. Katanoda, K. Matsuo and H. Fukanuma: Proc. Int. Therm. Spray Conf., (DVS, 2005) CD-ROM.
4) Y. Itoh, M. Saitoh and M. Tamura: J. Eng. Gas Turbines Power, Trans. ASME **122** (2000) 43–49.
5) S. Sampath, X. Y. Jiang, J. Matejicek, L. Prchlik, A. Kulkarni and A. Vaidya: Mater. Sci. Eng. A **364** (2004) 216–231.
6) T. C. Totemeier: J. Therm. Spray Technol. **14** (2005) 369–372.
7) T. H. Van Steenkiste, J. R. Smith and R. E. Teets: Surf. Coat. Technol. **154** (2002) 237–252.
8) H. Y. Lee, Y. H. Yu, Y. C. Lee, Y. P. Hong and K. H. Ko: J. Therm. Spray Technol. **13** (2004) 184–189.
9) J. Kawakita, T. Fukushima, S. Kuroda and T. Kodama: Corros. Sci. **44** (2002) 2561–2581.
10) S. Kuroda, Y. Tashiro, H. Yumoto, S. Taira and H. Fukanuma: J. Therm. Spray Technol. **10** (2001) 367–374.
11) G. N. Maniar: *Metals Handbook 9th Edition*, Vol. 2, Properties and Selection: Nonferous Alloys and Pure Metals (American Society for Metals, Materials Park, Ohio, 1979) pp. 525.
12) T. Wu, S. Kuroda, J. Kawakita, H. Katanoda and R. Reed: Proc. Int. Therm. Spray Conf., (ASM, 2006) CD-ROM.